Diamondoids as Molecular Building Blocks for Nanotechnology

Lahsen Assoufid[1], G. Ali Mansoori[2], Thomas F. George[3], Guoping Zhang[4]

[1]*Argonne National Laboratory, 9700 South Cass Avenue,*
Argonne, IL 60439, USA, Assoufid@aps.anl.gov

[2]*Departments of Bio and Chemical Engineering, University of Illinois at Chicago,*
Chicago, IL, 60612, USA, Mansoori@uic.edu

[3]*Office of the Chancellor and Center for Molecular Electronics, Departments of Chemistry,*
Biochemistry and Physics & Astronomy, University of Missouri–St. Louis,
St. Louis, MO 63121, USA, tfgeorge@umsl.edu

[4]*Department of Physics, Indiana State University,*
Terre Haute, IN 47809, USA, gpzhang@indstate.edu

ABSTRACT

Physical and chemical properties of diamondoids, which are organic compounds with unique structures and properties, are investigated as molecular building blocks (MBBs) for nanotechnology. Some methods and concepts in their role as MBBs in the formation of nanostructures including various aspects of self-assembly are introduced. Those include self-assembly using a solid surface, immobilization techniques for molecules on a solid support, DNA-directed self-assembly, self-assembly in liquid medium, and a host-guest chemistry approach. The applications of diamondoids in host-guest chemistry to construct molecular receptors by self-assembly process are presented. A combined experimental and theoretical effort to investigate the complicated structure-property relation of diamond-like and self-assembling organic nanostructures at the nanoscale level is presented. It is concluded that diamondoids are one of the best candidates for MBBs in molecular nanotechnology to design nanostructures with predetermined physicochemical properties.

1. INTRODUCTION

This paper reviews an ongoing combined experimental and theoretical effort to investigate the complicated structure-property relation of diamond-like and self-assembling organic nanostructures named "diamondoids" (adapted from the Greek for diamond) [1-9] at the nanoscale level by innovative experimental techniques and high-level materials simulation. A clear understanding of such a relation is essential for designing functional molecular gears for micro-machines and sensitive bionanosensors, and for developing new nanodrugs, just to name a few. Diamondoids exhibit fascinating properties, such as hardness and stability, which make them a potential candidate for nanorobots and nanogears. However, they are too large on the nanometer scale and too small on the micron scale for manipulation by conventional tools. Our proposed strategy, then, is to systematically develop reliable methodologies and set up a database for complicated molecular interactions that can accurately represent diamondoid organic nanosystems. Our combined experimental and theoretical investigations are proceeding in a stepwise fashion as follows:

i. Development of methodologies for applications of gas chromatography-mass spectrometry, atomic-force microscopy, and microelectrophoresis equipment to characterize and measure intermolecular forces of diamondoid organic nanostructures.

ii. Development of an intermolecular interaction database and models that can accurately represent the diamondoid organic nanosystems involved.

iii. Application of the derived intermolecular forces to the prediction of structural properties of diamondoid organic nanostructures.

2. BACKGROUND OF DIAMONDOIDS

Diamondoids were first discovered and isolated from Czechoslovakian petroleum in 1933 and are now found in many different crude oils, with varying concentrations and compositions. They have diamond-like fused-ring structures with the same structure as the diamond lattice – highly symmetrical and strain free. The rigidity, strength, and assortment of their three-dimensional shapes make them valuable molecular building blocks. The simplest of these polycyclic diamondoids is adamantane, followed by its homologues adamantane, tria-, tetra-, penta-, and hexamantane. The unique structure of adamantane is reflected in its highly unusual

physical and chemical properties, which can have many applications in nanotechnology. The carbon skeleton of adamantane comprises a cage structure that may be used for encapsulation of other compounds, i.e., in drug delivery. Because of this, adamantane and diamondoids in general are commonly known as **cage hydrocarbons**. In a broader sense, they may be described as saturated, polycyclic, cage-like hydrocarbons. The diamond-like term arises from the fact that their carbon atom structure can be superimposed upon a diamond lattice. The homologous polymantane series has the general molecular formula $C_{4n+6}H_{4n+12}$ where n = 1,2,3,… (n = 1 for adamantane). Each successively higher diamondoid family shows increasing structural complexity and varieties of molecular geometries.

Adamantane   Diamantane   Trimantane   Tetramantanes

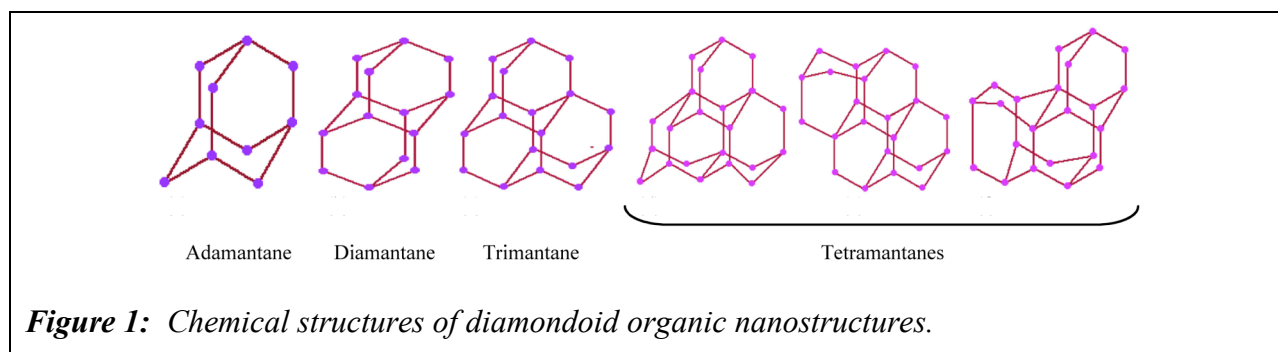**Figure 1:** *Chemical structures of diamondoid organic nanostructures.*

Figure 1 shows the chemical structures of adamantane, diamantane, and trimantane. Among the lower adamantologues, including adamantane, diamantine, and triamantane, each has only one isomer. Depending on the spatial arrangement of the adamantane units, higher polymantanes can have numerous isomers and non-isomeric equivalents. There are three possible tetramantanes, all of which are isomeric, respectively, as iso-, anti-, and skew-tetramantane depicted below. Anti- and skew-tetramantanes each posses two quaternary carbon atoms, whereas iso-tetramantane has three. There are seven possible pentamantanes, six being isomeric ($C_{26}H_{32}$) obeying the molecular formula of the homologous series and one non-isomeric ($C_{25}H_{30}$). For hexamantane, there are 24 possible structures: among them, 17 are regular cata-condensed isomers with the chemical formula ($C_{30}H_{36}$), six are irregular cata-condensed isomers with the chemical formula ($C_{29}H_{34}$), and one is peri-condensed with the chemical formula ($C_{26}H_{30}$).

It has been found that adamantane crystallizes in a face-centered cubic lattice, which is extremely unusual for an organic compound. The molecule therefore should be completely free

from both angular and torsional strain, making it an excellent candidate for various nanotechnology applications. At the beginning of growth, crystals of adamantane show only cubic and octahedral faces. The effects of this unusual structure upon physical properties are striking. Adamantane is one of the highest-melting hydrocarbons known (m.p. 269 ºC), yet it sublimes easily, even at atmospheric pressure and room temperature. Because of this, it again can have interesting applications in nanotechnology, which we are investigating. The phase transition boundaries (envelope) of adamantane need to be investigated and constructed. Predictable and diverse geometries are important features for molecular self-assembly and pharmacophore-based drug design. Incorporation of higher diamondoids in solid-state systems and polymers should provide high-temperature stability, a property already found for polymers synthesized from lower diamondoids.

Diamantane, triamantane, and their alkyl-substituted compounds, just as adamantane, are also present in certain petroleum fluids. Their concentrations in these fluids are generally lower than that of adamantane and its alkyl-substituted compounds. In rare cases, tetra-, penta-, and hexamantanes are also found in petroleum fluids.

Diamondoids offer the possibility of producing a variety of nanostructural shapes including molecular-scale components of machinery such as rotors, propellers, ratchets, gears, toothed cogs, etc. We expect them to have the potential for even more applications with molding and cavity formation characteristics due to their organic nature and their sublimation properties. The diverse geometries and varieties of attachment sites among higher diamondoids provide an extraordinary potential for the production of shape derivatives.
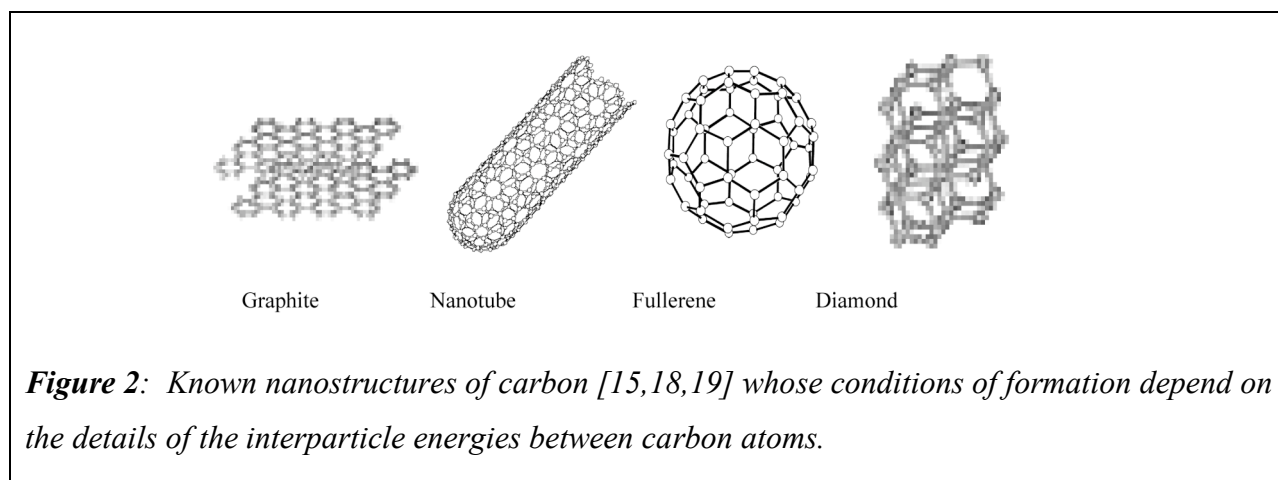
3. METHODOLOGY AND DISCUSSION

Our approach involves the development of methodologies for the application of atomic-force microscopy and microelectrophoresis equipment in order to construct a comprehensive approach for measuring the intermolecular forces that lead to the bonding of diamondoid organic nanostructures. We are building an intermolecular interaction database and models that can accurately represent the diamondoid organic nanosystems involved. Further, we are constructing molecular-based models for the prediction of structural characteristics resulting in organic diamondoids whether the outer shell is made of hydrogen or other elements. We first discuss our experimental progress below. This is followed by a discussion of our theoretical progress.

3.1. EXPERIMENTAL WORK

The interaction energies between atoms and simple molecules can be indirectly calculated through physical and thermodynamic measurements such as x-ray crystallography, light scattering, nuclear magnetic resonance spectroscopy, gas viscosity, thermal conductivity, diffusivity, and second virial coefficient data [10-15]. The existing models for intermolecular energies and forces are designed specifically for human-made systems. To control the matter atom-by-atom, molecule-by-molecule, and/or at the macromolecular level as is the aim of nanotechnology, it is necessary to know the exact intermolecular energies/forces between the particles under consideration. In the development of intermolecular energy/force models applicable for the study of nanostructures, which are at the confluence of the smallest of human-made devices and largest molecules of living systems, it is necessary to re-examine existing techniques and construct more appropriate intermolecular energy/force models and proper prediction techniques for structural characteristics.

Atomic-force microscopic data has been used to develop potential models to describe intermolecular interactions in condensed nanostructures such as C_{60} [16]. Although several studies have been published on the condensed phases of C_{60}, a comprehensive model that could allow the study of all carbon nanostructures (Fig. 2) is lacking [10-17].

Graphite   Nanotube   Fullerene   Diamond

Figure 2: *Known nanostructures of carbon [15,18,19] whose conditions of formation depend on the details of the interparticle energies between carbon atoms.*

Similarly, in order to predict the structural characteristics of diamondoid organic nanostructures (Fig. 1), accurate intermolecular potential energy data and appropriate models become necessary [17,20,21]. These compounds have diamond-like fused-ring structures

[http://www.uic.edu/~mansoori/Diamondoids.html] that can have many applications in nanotechnology [http://www.foresight.org/Conferences/MNT05/Abstracts/Drexabst.htm]. They have the same structure as the diamond lattice, i.e., highly symmetrical and strain free. The rigidity, strength, and assortment of their 3-d shapes make them valuable molecular building blocks.

As the size of diamondoids increases, the ratio of the number of carbon atoms to hydrogen atoms in the structure increases as well. For larger diamondoids, the inner structure will be mostly carbon, while the hydrogen molecules will cover the outer surface. It is possible to replace the outer hydrogens with other elements to increase the intermolecular interactions between various diamondoids.

### 3.1.1. Atomic-force microscopy (AFM) measurements

AFM is a unique tool for studying intermolecular energies/forces. Unlike traditional microscopes, AFM does not use optical lenses and therefore provides a very high-resolution range of various sample properties [22-24]. It operates (Fig. 3) by scanning a very sharp tip across a sample, which 'feels' the contours of the surface in a manner similar to a stylus tracing across the grooves of a record. In this way, it can follow the contours of the surface and so create a topographic image, often with subnanometer resolution [25-30]. This instrument also allows researchers to obtain information about the specific forces between and within molecules on the surface. By its very nature, AFM is extremely sensitive to intermolecular forces and has the ability to measure force as a function of distance (see Fig. 4).
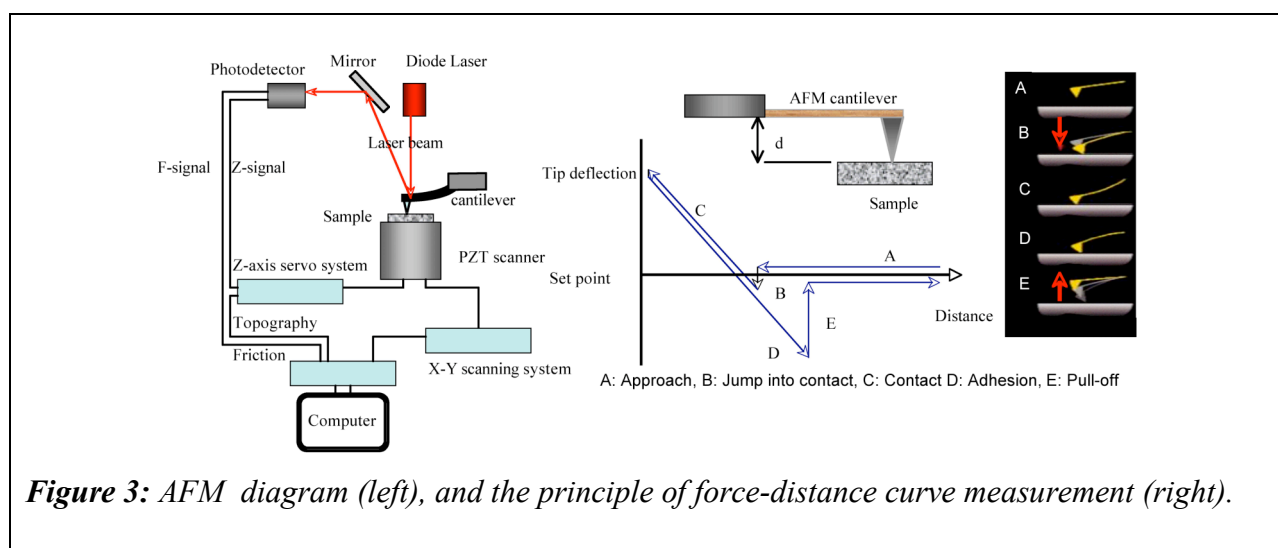
Figure 3: *AFM diagram (left), and the principle of force-distance curve measurement (right).*

In AFM measurements, the relative displacement of a tip is measured with high precision (Fig. 3), whereas the absolute separation distance between the tip and a surface remains to a large degree indefinite. In addition, the force-distance curves do not lead immediately to intermolecular interaction potentials. Because of this, the recovery of the reliable force-distance curves and interaction potentials through direct AFM measurements encounters interpretation problems [30-32]. Let us describe the manner in which we are resolving these problems:

(1) One can fit the experimental force-distance curve using its asymptotes at large separation distances when the specific properties of the nanostructures under investigation do not play an important role, and when a force-distance relation can be described as the van der Waals force between the macrobodies of appropriate shape. This method, however, is not fully exact as the forces in an asymptotic region are too small. Therefore, it is necessary to find potentials; to do this, a comprehensive mathematical modeling will be performed as described in the theoretical section below. We are considering several theoretical intermolecular potential functions maximally adapted for the molecules under consideration and are computing a set of force-distance curves given by these potentials. These theoretical curves are being fitted to the experimental curve, where the best fit determines the appropriate potential for the description of the experimental situation under consideration. In fact, the search for potential functions in this way is equivalent to a solution of the inverse problems, which are well known from mathematics.

(a)   (b)
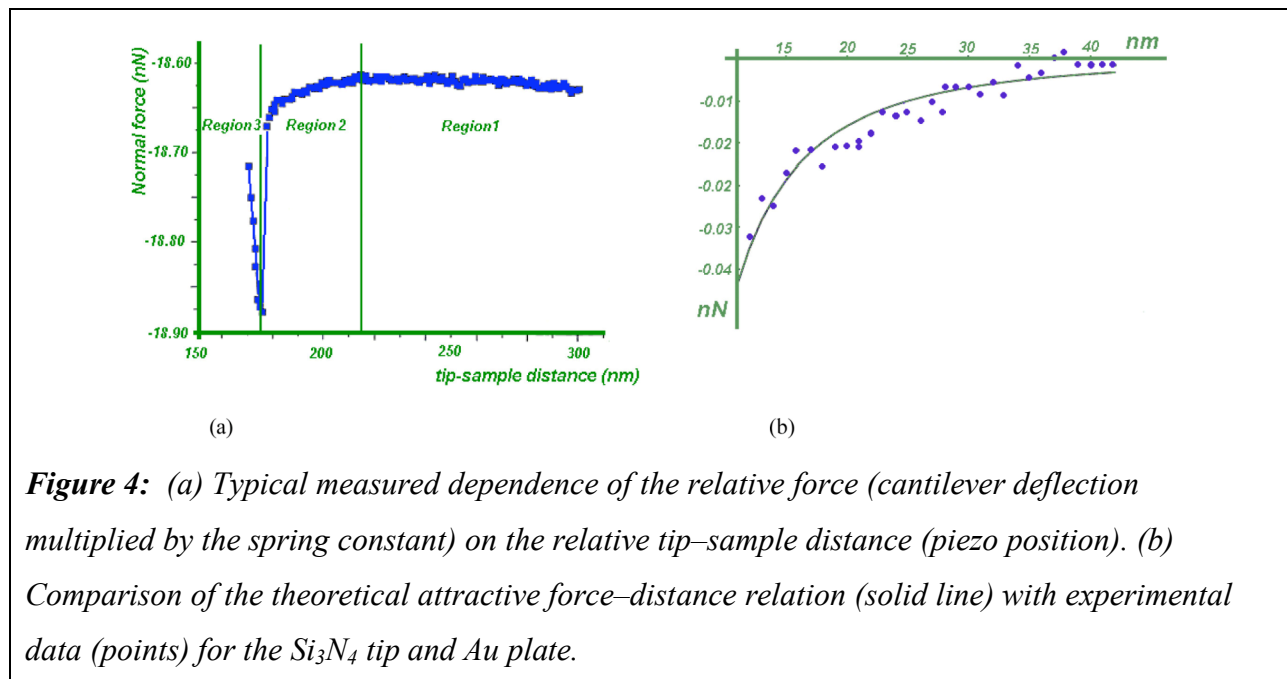
Figure 4: *(a) Typical measured dependence of the relative force (cantilever deflection multiplied by the spring constant) on the relative tip–sample distance (piezo position). (b) Comparison of the theoretical attractive force–distance relation (solid line) with experimental data (points) for the Si_3N_4 tip and Au plate.*

(2) Another technique that we are using does not rely on the asymptotic region of large separations, but rather considers the true separation distance as an additional parameter to be determined by the fit of different theoretical force-distance curves, following from different potential functions, to an experimental curve. This method is a bit more labor intensive but may lead to more reliable results.

The basic method being developed enables us to obtain AFM measurement data containing information about the interaction energy between macromolecules. This data is in turn used for the mathematical simulations and modeling of reliable intermolecular potentials. The interparticle interaction potential energy between molecules is generally denoted by $\phi = \phi_{rep} + \phi_{att}$, where r is the intermolecular distance, ϕ_{rep} is the repulsive interaction energy, and ϕ_{att} is the attractive interaction energy, as depicted by Fig. 5 below.

*Figure 5: Pair interaction between molecules.*
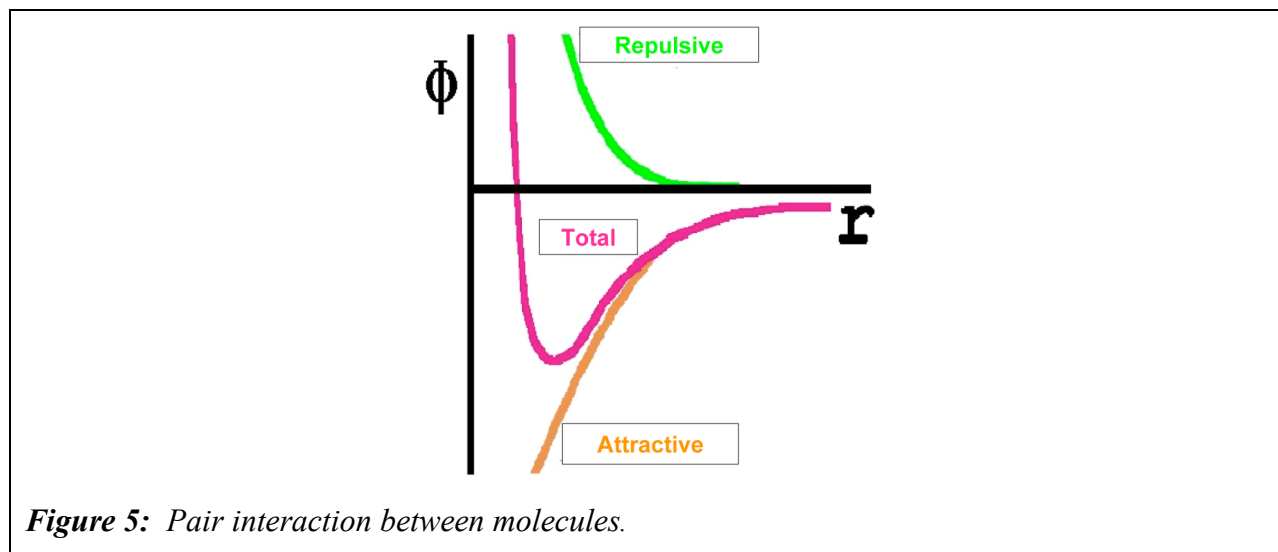
Recent progress in AFM technology is allowing the measurement of inter- and intramolecular forces at the level of individual molecules. Also, making microelectrophoretic measurements of the zeta potential allows us to calculate the total interparticle energies indirectly.

3.1.2. Microelectrophoretic measurements

The movement of charged nanoscale particles in an electric field is termed microelectrophoresis, which is a novel approach to nanoscale analysis of organic nanostructures. This is of practical importance in intermolecular interaction research, involving the movement of particles under the influence of a carefully controlled electrical field to measures a nanoparticle's

zeta potential. This potential is the overall charge that a particle acquires in a specific medium and is a measure of the magnitude of the repulsion or attraction energies between particles. A properly-executed microelectrophoretic measurement can be highly effective in providing the data necessary to test the intermolecular force models that will be generated by AFM. When nanoparticles are dispersed in a liquid medium, they attract one another due to attractive forces. By adjusting the properties of the medium, the nanoparticle surface charge can be manipulated such that the repulsive electrical double layer (Fig. 6) is eliminated around the particles.

Figure 6: *Attractive and electric double layer repulsive energies around dispersed nano-particles.*
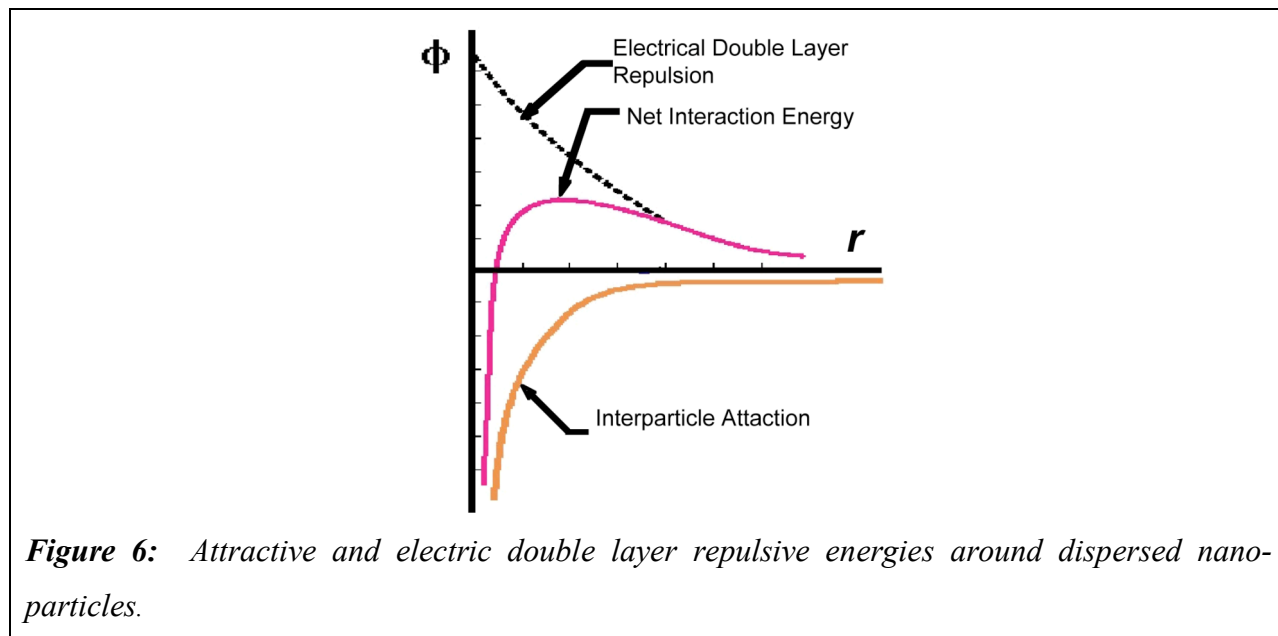
The magnitude of this attractive energy can be measured via the zeta potential. From the combined AFM and microelectrophoretic measurements, accurate force-distance curves can be obtained. Non-contact AFM is being used for attractive interaction force measurements, and contact AFM will be used for repulsive force measurements. Intermittent-contact AFM is more effective than non-contact AFM for imaging larger scan sizes. From the relation between the force and distance, an interparticle force *vs* distance curve can be created.

Our work microelectrophoretic measurements involve a microelectrophoretic model 501 LASER ZEE METER™ (Fig. 7), modified for applications in both aqueous and organic media. The experimental application of the AFM is not sufficient if it is not supplemented by serious theoretical work. The combined power of the AFM method and theoretical modeling enables us to determine intermolecular interaction energies for nanostructures to high accuracy.
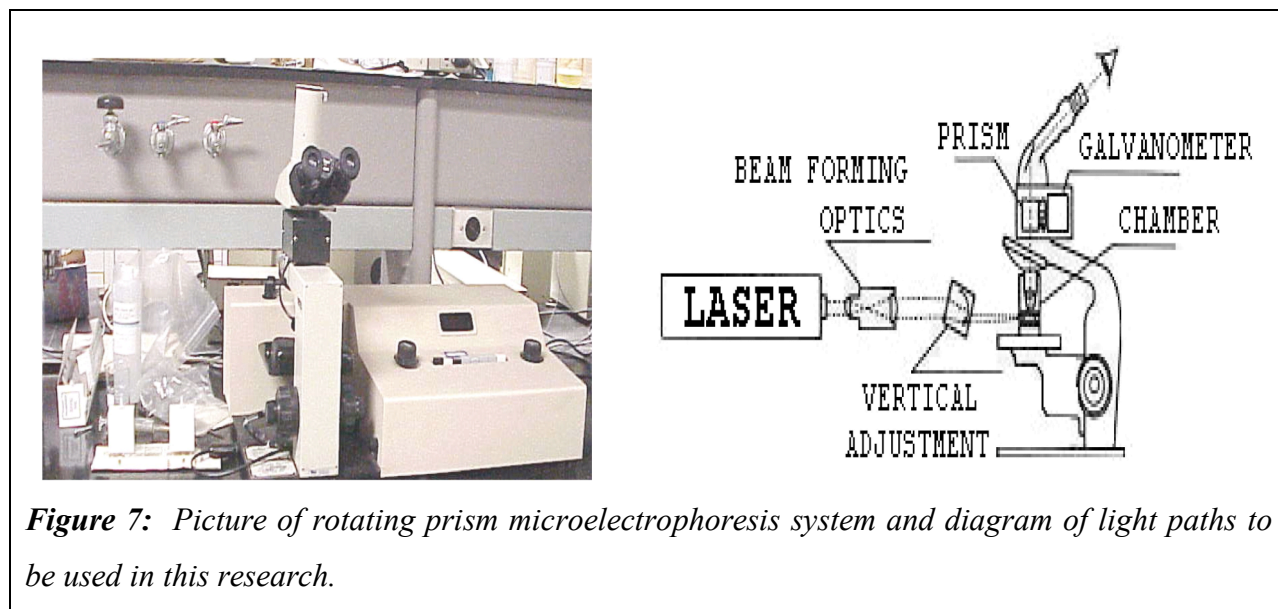
Figure 7: *Picture of rotating prism microelectrophoresis system and diagram of light paths to be used in this research.*

3.2. THEORETICAL RESULTS AND DISCUSSION

Interparticle energies are known to be orientation-dependent and are a sum of repulsive, London dispersion, hydrogen bonding, and electrostatic energies, i.e., $\phi\,(r, \theta_i, \theta_j, \varphi) = \phi_{rep} + \phi_{disp} + \phi_{dipole} + \phi_{quad.} + \phi_{ind.dipole} + \ldots$, where r is the separation of the two bodies, θ_i, θ_j are the angles between the axes of the two molecules i and j and the line joining their centers, and φ is the azimuthal angle between the planes containing these areas. For neutral and spherically symmetric molecules when the separation r is very small, an exponential repulsive term $\phi_{rep} = \alpha \cdot exp(-\beta r)$ dominates, and the potential is strongly positive. Hence, ϕ_{rep} describes the short-range repulsive potential due to the distortion of the electron clouds at small separations. For neutral and spherically symmetric molecules when the separation r is large, the London dispersion forces dominate. The total interaction force is $F = -[\partial\phi(r)/\partial r]_{\theta i \theta j, \varphi} = F_{rep} + F_{att}$.

In systems consisting of many different kinds of particles (atoms, molecules), macroscopic properties can be predicted using statistically averaged (effective) intermolecular potential energy functions. It must be pointed out that there is an acute need for accurate intermolecular potential energy models that can be used for the prediction of structural properties of diamondoid nanostructures [2,8,33]. The emphasis of nanotechnology presently is placed on nanosolid and nanoliquid systems. The question of how certain structural features show up in systems with, say 50-1000 particles, can be answered effectively with a knowledge of

appropriate potential models in conjunction with the structure factor and other molecular-based characteristics [2,8,33].

In order to avoid the barrier of the thermodynamic limit, certain formalisms must be applied in deriving the structure factor and correlation functions, which can be applicable to small as well to other containable systems. We have constructed a basic molecular-based model for diamondoid phase transitions, micelles, and micelle-coacervate formations [20,33].

Theoretically, there are tremendous challenges and opportunities. The challenges exist because there is no simple way to extract potential energy surfaces from force measurements. A given potential energy surface is a function of the many coordinates of the nanoparticles. Especially for large molecules, there may be many different potential surfaces corresponding to the same force measurement. We start with some simple molecules to see whether the first-principles calculation can reveal the essential mechanisms involved or not.

The advantage of these theories is that they are normally parameter free. This will be an independent check of our experimental results and the model potentials. Moreover, with more than 50 years of development, these theories have become quite sophisticated and have strong reliability and predictability. They essentially can treat all kinds of atoms and molecules. For instance, recently we used *ab initio* theory to simulate the reaction path for a retinal molecule in rhodopsin [34] (see Fig. 8).

We have shown that not only the ground state [Fig. 9(a)] but also the excited states [Fig. 9(b)] can be calculated precisely. Figure 9(a) shows that with the change in the angle φ around C11-C12, the potential energy changes dramatically. There are several minima and maxima along the rotational path. To get such an accurate result, we have included the basis states with the diffusive components in order to represent the atomic orbitals. Figure 9(b) shows that the excited states undergo a similar change, but there are several differences with the transition matrix elements. In particular at $\varphi = 0$ or 180°, the transition matrix elements are very large. However, in between the elements are very small. This explains the funneling effect that has been seen in experiments, which shows the high efficiency of the isomerization process.
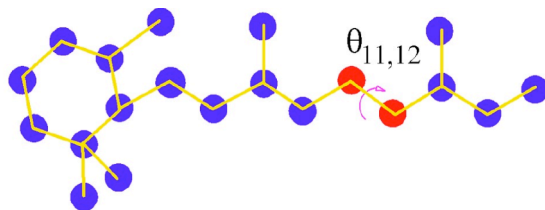
Figure 8: *Rhodopsin segment. Isomerization occurs around the bond 11-12 with angle $\theta_{11,12}$.*

It is well known that the potential resulting from electrons is much more difficult to treat than that from atoms because the electron density is extremely sensitive to structural changes and external perturbations. Experimentally, the electronic contribution is often very difficult to probe since an external intervention will affect the intrinsic electron distribution substantially. Theoretically, we have the flexibility to calculate these intrinsic properties.
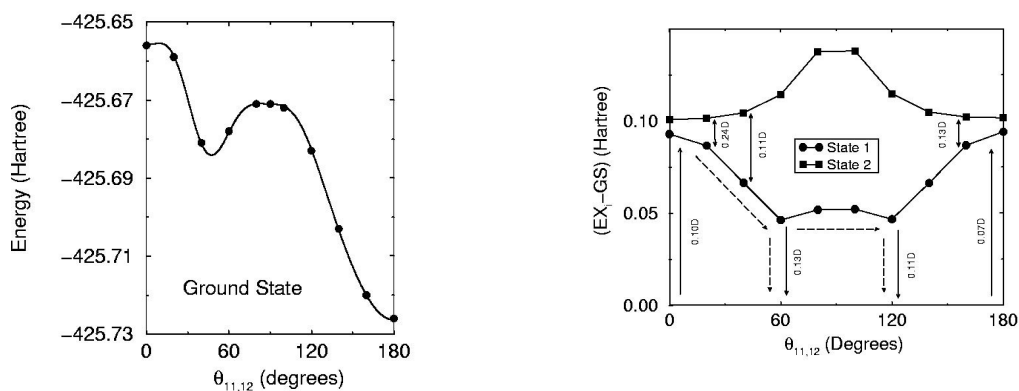
Figure 9. *(Left) Ground-state potential versus angle $\theta_{11,12}$ in a segment of rhodopsin. (Right) Potential for the excited state vs the angle around the bond 11-12. Importantly, the transition matrix elements are also accurately obtained.*

4. CONCLUSIONS

Physical and chemical properties of diamondoids are investigated as molecular building blocks (MBBs) for nanotechnology. A combined experimental and theoretical effort to investigate the complicated structure-property relation of diamond-like and self-assembling organic nanostructures at the nanoscale level is presented. Our experimental approach involves the application of atomic-force microscopy and microelectrophoresis equipment in order to

construct a comprehensive approach for measuring the intermolecular forces that lead to the bonding of diamondoid organic nanostructures. The methodology of exploiting AFM and microelectrophoresis to be build a theoretical model to predict structural properties of these diamondoid organic nonotructures was described.

ACKNOWLEDGMENTS

REFERENCES

1. Internet website: *http://tigger.uic.edu/~mansoori/Diamondoids.html.*

2. Internet website: *http://www.foresight.org/Conferences/MNT05/Abstracts/Drexabst.htm.*

3. Baroody, E. E. and Carpenter, G. A., Rpt. Naval Ordnance Systems Command Task No. 331-003/067-1/UR2402-001 for Naval Ordnance Station, Indian Head, Maryland (1972), pp. 1-9.

4. Boyd, R. H. *et al., J. Phys. Chem.* **75**, 1264 (1971).

5. Clark, T. *et al., J. Am. Chem. Soc.* **101**, 2404 (1979).

6. Jochems, R., Dekker, H., Mosselman, C., Somesen, G., *J. Chem. Thermodyn.* **14**, 395, (1982).

7. Mansoori, G. A., *J. Petrol. Science & Eng.* **17**, 101 (1997).

8. Vazquez Gurrola, D., Escobedo, J. and Mansoori, G. A., "Characterization of Crude Oils from Southern Mexican Oil Fields," in *EXITEP 1998 Proceedings* (Mexico City, Mexico, 1998).

9. Westrum, Jr., E. F., *J. Phys. Chem. Solids* **18,** 83 (1961).

10. Rafii-Tabar, H. and Mansoori, G. A., "Interatomic Potential Models for Nanostructures," (2003) to be published. Preprint can be downloaded from *http://www.uic.edu/labs/trl/NanostructurePotentialModels.pdf*.

11. Gans, W. and Boeyens, J. C. A. (Eds.) *Intermolecular Interactions* (Plenum, New York, 1998).

12. Stone, A., *The Theory of Intermolecular Forces* (International Series of Monographs on Chemistry, No. 32 (Oxford University Press, Oxford, 1997).

13. Terakura, K. and Akai, H., *Interatomic Potential and Structural Stability*, Proceedings of the 15th Taniguchi Symposium, Kashikojima, Japan (Springer Series, 1993).

14. Edalat, M., Pang, F., Lan, S. S. and Mansoori, G. A., *Int. J. Thermophysics* **1**, 177 (1980).

15. Boudh-Hir, M. E. and Mansoori, G. A., *Physica* A **179**, 219 (1991). See also Escobedo, J. and Mansoori, G. A., *AIChE J.* **44**, 2324 (1998).

16. Gamba, Z., *J. Chem. Phys.* **97,** 553 (1992).

17. Nalwa, H. S. (Ed.), *Handbook of Nanostructured Materials and Nanotechnology* (Academic Press, San Diego, 1999).

18. Collins, P. G. *et al.*, *Science* **278,** 100 (1997).

19. Roco, M. C., Williams, R. S. and Alivisatos, P. (Eds.), *Nanotechnology Research Directions: IWGN Workshop Report* (Kluwer, Dordrecht, 2000).

20. Sanchez, J. H. P. and Mansoori, G. A., *J. Petrol. Sci. & Tech.* **16**, 377 (1998).

21. Stu, S. I., LeBonheur, V., Wlaker, K., Li, L.S., Huggins, K. E., Keser, M. and Armstutz, A., *Science* **276**, 384 (1997).

22. Binnig, G., Quate, C. F. and Gerber, Ch., *Phys. Rev. Lett.* **56**, 930 (1986).

23. Hutter, J. L., and Bechhoefer, J., *J. Appl. Phys.* **73**, 4123 (1993).

24. Hutter, J. L. and Bechhoefer, J., *J. Vac. Sci. Technol. B* **12**, 2251 (1994).

25. Derjaguin, B. V., Rabinovich, Y. I. and Churaev, N. V., *Nature* **272**, 313 (1978).

26. Diehl, A., Babosa M. C. and Levin, Y., *Europhys. Lett.* **53,** 86 (2001).

27. Ducker, W. A., Senden, T. J. and Pashley, R. M., *Nature* **353**, 239 (1991).

28. Ducker, W. A., Senden, T. J. and Pashley, R. M., *Langmuir* **2**, 1831 (1992).

29. Hugel, T. and Seitz, M., *Macromol. Rapid Commun.* **22**, 989 (2001).

30. Zanette, S. I., Caride, A. O., Nunes, V. B., Klimchitskaya, G. L., Freire, Jr., F. L. and Prioli, R., *Surf. Sci.* **453**, 75 (2000).

31. Blagov, E. V., Klimchitskaya, G. L., Lobashov, A. A. and Mostepanenko, V. M., *Surf. Sci.* **349**, 196 (1996).

32. Blagov, E. V., Klimchitskaya, G. L. and Mostepanenko, V. M., *Surf. Sci.* **410**, 158 (1998).

33. Priyanto, S., Mansoori, G. A. and Suwono, A., *Chem. Eng. Sci.* **56**, 6933 (2001).

34. Zhang, G. P., Zong, X. F. and George, T. F., *J. Chem. Phys.* **110**, 9765 (1999).